Parameters and Volt-Ampere Ratings of a Synchronous Motor Drive for Flux-Weakening Applications

Nicola Bianchi and Silverio Bolognani

***Abstract*— This paper deals with the selection of the motor parameters and the inverter power ratings for a permanent-magnet (PM) synchronous motor drive in order to meet a given flux-weakening torque versus speed characteristic. Appropriate combinations of stator PM flux linkage, d- and q-axis inductances, and inverter current rating at a given voltage are derived, in normalized values, as functions of the specified flux-weakening speed range and torque limits. By means of these sets of data, the drive designer can easily individuate and compare all the suitable synchronous motors (defined by the d- and q-axis inductances and flux linkage) and the related inverter volt-ampere ratings, for the desired flux-weakening performance. Therefore, this paper can be considered a synthesis work rather than an analysis one and can profitably be used for an optimal design of a synchronous motor drive.**

***Index Terms*—Flux weakening, motor design, synchronous motor drives.**

NOMENCLATURE

I	Rated motor and inverter current (A).
I_dI_q	d-axis and q-axis current components (A).
L_dL_q	d-axis and q-axis inductances (H).
p	Number of pole pairs.
T	Motor torque (N · m).
T_b	Rated motor torque (N · m).
T_{fw}	Flux-weakening torque (N · m).
V	Rated motor and inverter voltage (V).
γ_b	Current angle at base operating point (rad).
Λ_m	Stator PM flux-linkage (V · s).
ξ	Saliency ratio.
Ω	Angular frequency and electrical speed (rad/s).
Ω_b	Base electrical speed (rad/s).
Ω_{fw}	Maximum flux-weakening operating electrical speed (rad/s).
Ω_m	Mechanical speed (rad/s).
$\Omega_{\max}$	Maximum drive electrical speed (rad/s).
Ω_p	Maximum constant volt-ampere electrical speed (rad/s).

Small letters are used for normalized quantities.

Manuscript received February 23, 1996; revised December 18, 1996. Recommended by Associate Editor, D. A. Torrey.

The authors are with the Department of Electrical Engineering, University of Padova, 35131 Padova, Italy.

Publisher Item Identifier S 0885-8993(97)06407-7.

I. INTRODUCTION

IN THE LAST years, variable-speed applications and operating limits for interior permanent-magnet (IPM), surface permanent-magnet (SPM), and reluctance (REL) synchronous motors obtained a great interest. Steady-state analysis and control methods for variable-speed operation above the base speed, namely in the flux-weakening region, of synchronous motor drives (SMD) with current-regulated inverters are described in several papers. Early works on flux-weakening operation of SMD deal with the analysis and control of IPM motors [1]–[3]. Then SPM motors [4] and both types of permanent-magnet (PM) motors [5]–[8], [11] were investigated. REL motors are considered in [9] and [10], while the operation of the three types of SMD is analyzed and compared in [12] and [13].

All the drives exhibit a constant torque region, from zero to the base speed, with increasing voltage. Then, a decreasing torque region follows, with a constant voltage, which extends up to the maximum operation speed. The high-speed constant voltage operation is accomplished by reducing the stator PM flux linkage through an appropriate stator current distribution and thus it is generally called "flux-weakening region."

In the aforementioned papers, the analysis is usually performed by starting from given motor parameters and inverter size and then the resulting drive performance is predicted. Conversely, the purpose of this paper is to select the motor parameters (and therefore the motor type) and the inverter volt-ampere ratings of an SMD, in order to meet a desired flux-weakening torque versus speed specification. In particular all the combinations of stator PM flux linkage and d- and q-axis inductances (which together define the motor type), as well as the inverter current rating at a given voltage, are derived for fixed flux-weakening speed range and torque limits. By means of these sets of data, the drive designer can easily individuate and compare the different suitable synchronous motors and related inverter sizing, for any specified flux-weakening performance. For these reasons, this paper can be considered a synthesis work rather than an analysis one and it can be profitably used for an optimal design of an SMD for a given torque-speed curve.

II. STEADY-STATE SMD EQUATIONS

The steady-state equations of the SMD operation are studied with some simplifying assumptions: 1) the winding resistance

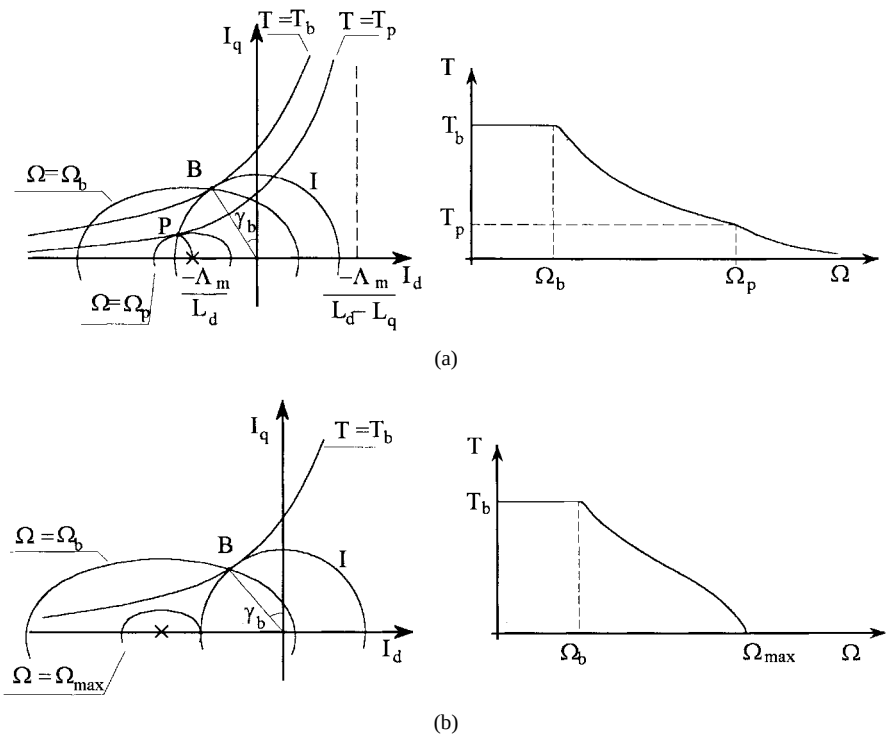

Fig. 1. Circle diagrams of IPM motor drives.

is neglected; 2) the iron permeability is considered infinite so that the saturation effects are not taken into account; 3) the iron losses are neglected; and 4) the PM irreversible demagnetization caused by the stator reaction is not considered, assuming a PM material with an appropriate coercive force and/or thickness.

In the general form of the synchronous motor equations, both the effect of the PM and that of the rotor saliency have to be considered, as in an IPM machine. By using a synchronous d-q reference frame with the d-axis coincident with the PM polar axis, the steady-state torque T developed by an IPM motor is

$$T = \tfrac{3}{2}[\Lambda_m I_q + (L_d - L_q) I_q I_d]. \tag{1}$$

Two terms in the torque (1) can be recognized: the first one is the PM torque term and the second one is the reluctance torque term. For this reason, an IPM motor can be interpreted as a combination of an SPM motor $(L_d = L_q)$ and an REL motor $(\Lambda_m = 0)$ and then its equations can be used for an unified study of an SMD.

An analysis of the IPM motor operation above base speed can readily be carried out using the circle diagram in the I_d-I_q plane [6], [12]. In that plane, (1) defines, for each torque T, a hyperbola whose asymptotes are the axis $I_q = 0$ and the vertical straight line $I_d = -\Lambda_m/(L_d - L_q)$. The latter lies in the positive I_d semiplane, since all the IPM motors exhibit $L_d < L_q$. The rated motor current and voltage must be within the inverter capabilities. In this study the rated motor quantities are assumed to be exactly coincident with the inverter limits V and I. By considering the inverter capabilities, the current limit defines a circle in the $I_d - I_q$ plane, centered in the plane origin, and given by

$$I^2 = I_d^2 + I_q^2 \tag{2}$$

and the voltage limit defines an ellipse, centered in $(-\Lambda_m/L_d, 0)$, with the ellipticity equal to the saliency ratio $\xi = L_q/L_d$, and the major axis equal to $2V/(\Omega L_d)$, and expressed by

$$V^2 = \Omega^2[(\Lambda_m + L_d I_d)^2 + (L_q I_q)^2] \tag{3}$$

where Ω is the operating angular frequency or electrical speed. The latter is related to the mechanical speed Ω_m by $\Omega = p\Omega_m$. It is easy to prove that the center of the ellipses represents the steady-state three-phase short-circuit operating condition of the machine. Equation (3) applies also to SPM and REL motors by putting $L_q = L_d$ and $\Lambda_m = 0$, respectively.

Fig. 1 shows two circle diagrams with two different short-circuit current levels. The rated current limit circle, two voltage limit ellipses (drawn for rated voltage and two different motor speeds), and some constant torque hyperbolas are shown. Operating points which lie outside either the current limit circle or the voltage limit ellipse, do not comply with drive voltage and current limitations. Rated torque T_b is the maximum torque which can be obtained by rated current. The base speed Ω_b (in electrical rad/s) is the speed at which the drive delivers rated torque with rated voltage. The two quantities, T_b and Ω_b, are associated with the hyperbola and the ellipse crossing the point B in Fig. 1, where the hyperbola is tangent to the current limit circle. In the paper it is assumed $V \geq \Omega_b \Lambda_m$ so that operation at base speed and null currents is allowed, i.e., the origin of the I_d-I_q plane is inside the voltage limit ellipse related to the base speed.

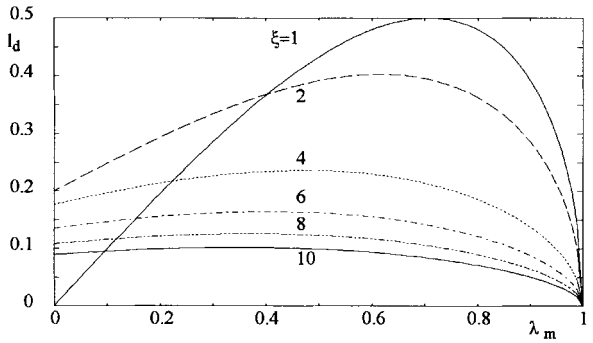

(a)

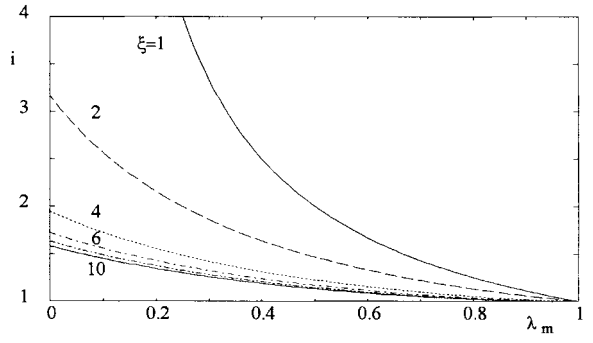

(b)

Fig. 2. d-axis inductance and rated current of an IPM motor drive, as functions of λ_m and ξ with the same unitary base speed, rated torque, and rated voltage.

An SMD as described in Fig. 1 has three operating regions.

I) Constant Torque Region: This occurs below and up to the base speed Ω_b; the torque limit is constant and equal to the rated torque, delivered by constant I_d and I_q, chosen so that maximum torque-to-current ratio is achieved. Operation in the constant torque region, under rated torque and current, is described by point B in Fig. 1.

II) Flux-Weakening, Constant Volt-Ampere Region: Operation in this region is limited by the rated current and the rated voltage. The operating point under these limit conditions is the intersection of the current limit circle with the voltage limit ellipse. In the case of Fig 1(a), the point moves from B to P, along the current limit circle, as the speed increases from Ω_b to Ω_p the latter being therefore the maximum speed of the flux-weakening constant volt-ampere region. In the operating point P, the torque hyperbola is tangent to the voltage limit ellipse. Thus, the drive exhibits in P the maximum torque-to-voltage ratio. If the center of the ellipses is outside the current limit, as in Fig. 1(b), the operating point P does not exist: the constant volt-ampere region ends at the operating point of the current circle which lies on the I_d-axis, where a null torque and the maximum drive speed $\Omega_{\max}$ occur.

III) Flux-Weakening, Decreasing Volt-Ampere Region: This operating region turns out only when the center of the ellipses is inside the current limit as in Fig. 1(a). In that case, above Ω_p the drive performance limits are defined by the maximum torque-to-voltage locus which links P with the ellipse center, where the drive operates at infinite speed ($\Omega_{\max} = \infty$).

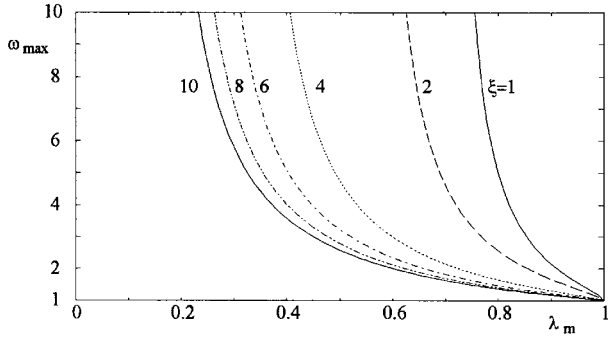

Fig. 3. Maximum drive speed of the drive of Fig. 2.

In this paper the design of an SMD is faced with the aim of individuating the motor parameters (flux linkage and d-q axis inductances) and the inverter volt-ampere ratings, such that the drive exhibits a rated torque T_b at base speed Ω_b and a prefixed flux-weakening operation range, defined by the torque T_{fw} at the maximum desired flux-weakening operating speed Ω_{fw}. Both the cases of Ω_{fw} lower and higher than Ω_p are considered. Therefore the paper generalizes the results presented in [14], in which the same problem has been solved under the assumptions that region III does exist and by putting $\Omega_{fw} = \Omega_p$.

The drive data are obtained from the SMD equations (1)–(3) by imposing the torque T_b at speed Ω_b together with the torque T_{fw} at speed Ω_{fw}. All the data are given in normalized values (small letters) referred to the base quantities defined in the Appendix, so that the obtained results can be extended to motors of any rated power. Moreover, the use of normalized values allows an easy comparison between different SMD sizing but with equal flux-weakening performance. The inverter voltage limit, rated torque and base speed, are among the base quantities, so that the normalized rated voltage is $v = 1$, and similarly the normalized rated torque and base speed are $t_b = 1$ and $\omega_b = 1$, respectively. Since it has been assumed $V \geq \Omega_b \Lambda_m$, it results $\lambda_m \leq 1$.

For the sake of convenience and an easy use of the results, the motor drive data are reported in the paper in several figures. By means of these figures, when the desired flux-weakening torque t_{fw} and speed ω_{fw} are prefixed, the drive designer can select the most suitable SMD, by individuating the appropriate motor parameters (d- and q-axis inductances and flux linkage) and the inverter current rating. An effective procedure for designing the motor according to the inductances and flux linkage data is proposed in [15].

III. SMD Base Speed Operation

As stated in Section II, SMD operation at base speed is described by the operating point B in Fig. 1, which is the point where the current limit circle is tangent to the rated torque hyperbola. In addition, B is the crossing point between the previous curves and the voltage limit ellipse drawn for base speed Ω_b. The d-axis inductance and the rated current of a drive operating in B can be found, as functions of the flux linkage λ_m and saliency ratio ξ, by solving (1) and (3) for rated torque and voltage, also base speed, together with

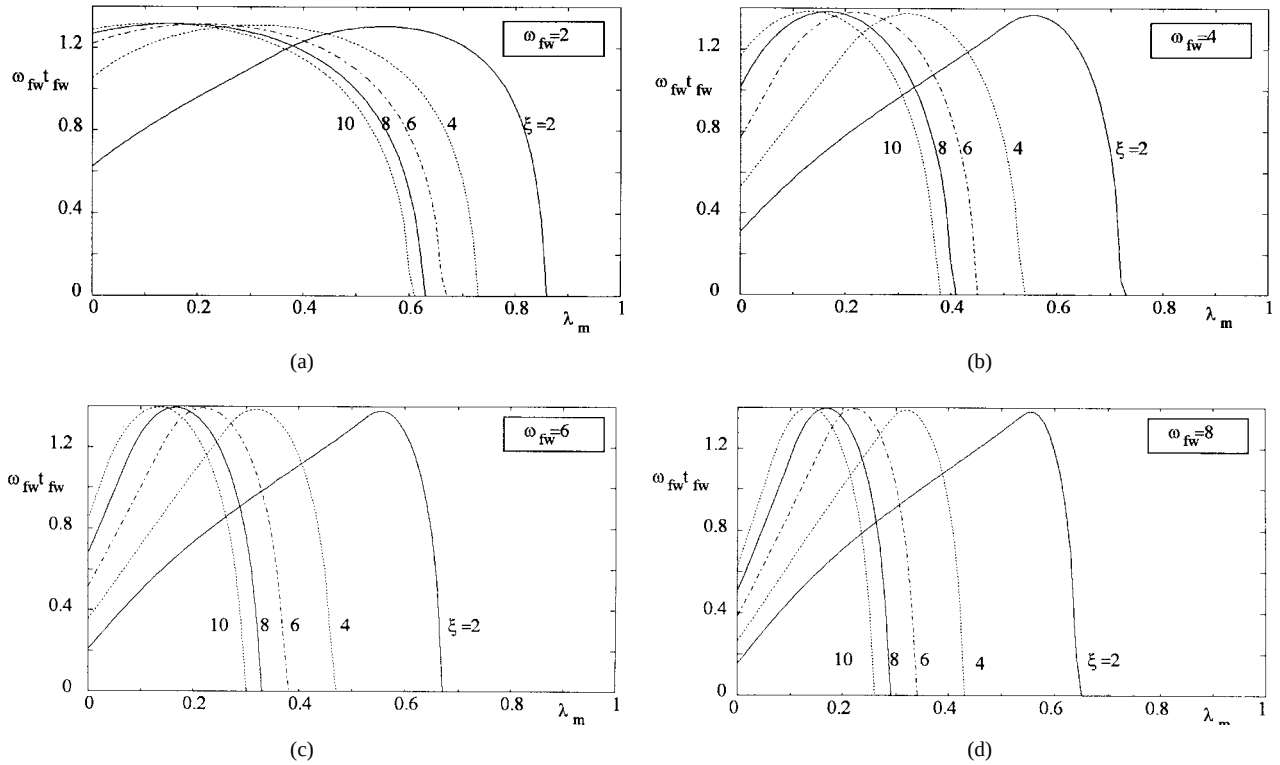

Fig. 4. Flux-weakening power of the drive of Fig. 2, as functions of λ_m and ξ and for different ω_{fw}.

the equation obtained by imposing the maximum torque-to-current ratio. All these equations are expressed hereafter in normalized form.

From (1), the normalized torque becomes

$$t_b = \lambda_m i \cos\gamma_b - 1_d(1-\xi)i^2 \frac{\sin 2\gamma_b}{2} \tag{4}$$

while, from (3), the voltage is

$$v^2 = \omega_b^2[(\lambda_m - 1_d i \sin\gamma_b)^2 + (1_d \xi i \cos\gamma_b)^2]. \tag{5}$$

In (4) and (5) the angle γ_b, defined in Fig. 1, is given by

$$\sin\gamma_b = \frac{\lambda_m - \sqrt{\lambda_m^2 + 81_d^2(1-\xi)^2 i^2}}{41_d(1-\xi)i} \tag{6}$$

obtained by equating to zero the derivative of the torque-to-current ratio with respect to γ_b.

By fixing $t_b = 1, v = 1, \omega_b = 1$ in (4) and (5), the normalized d-axis inductance l_d and rated current i are obtained, as functions of λ_m and ξ. Because of the nonlinearity of the system of (4) and (5), the solution is reached by a numerical method. The results are shown in Fig. 2. In the particular cases of an SPM motor and an REL motor, the base-speed operation is described by the curve $\xi = 1$ and by the axis $\lambda_m = 0$, respectively. For these cases, (4) and (5) can be solved analytically and the quantities l_d and i can be also given in closed form, as described in Section VI.

In Fig. 2(a) the normalized inductance l_d is reported as a function of flux linkage λ_m, for different values of the saliency ratio ξ. In a similar way, the corresponding normalized current i, is reported in Fig. 2(b). By means of Fig. 2 one can individuate all the possible SMD configurations to achieve a given base-speed operating point. It is worth noticing that the current rating decreases as ξ and λ_m increase. However, a high ξ generally implies a complicated and expensive rotor structure, while a high λ_m may imply a high cost of the PM. Thus, the combination of the reluctance and PM features in the motor design have to be carefully balanced.

IV. SMD Flux-Weakening Maximum Speed

The flux-weakening operation is accomplished above base speed. The flux-weakening speed range extends till the drive operating point in the I_d-I_q plane can be maintained inside both the voltage and current limits.

Two cases are possible, according to whether the PM flux linkage Λ_m is lower or greater than $L_d I$, as previously mentioned. In the first case, the center of the ellipses is inside the current limit and therefore no electrical limitations exist to the maximum speed of the drive, as in Fig. 1(a). In the second case the center of the ellipses is outside the current limit, so that operating region III does not exist and the drive has a finite maximum speed $\Omega_{\max}$ at which the torque is zero, as in Fig. 1(b). From the figure, one realizes that at the maximum speed, the voltage limit ellipse is tangent to the current limit circle, and only one operating point is thus allowed.

The maximum speed is obtained by imposing $I_d = -I$ and $I_q = 0$ in (3), yielding to

$$\Omega_{\max} = \frac{V}{\Lambda_m - L_d I}. \tag{7}$$

The speed (7) of an IPM motor drive, in normalized value $\omega_{\max}$, can be expressed as a function of the PM flux linkage λ_m for different saliency ratios ξ, by using l_d and i given

TABLE I
DIFFERENT SMD DESIGNS FOR $t_{fw} = 0.2$ AND $\omega_{fw} = 4$

	type	λ_m	ξ	l_d	l_q	i	ωmax	ellipses centre
a	SPM	0.803	1	0.479(*)	0.479(*)	1.25	4.83	out
b	REL	0	6.2	0.132	0.817	1.71	∞	in
c	IPM	0.495	4	0.236	0.943	1.23	4.87	out
d	IPM	0.080	4	0.193	0.773	1.76	∞	in
e	IPM	0.693	2	0.397	0.794	1.23	4.86	out
f	IPM	0.210	2	0.298	0.596	2.12	∞	in

(*) including external inductances

in Fig. 2. The values of $\omega_{\max}$ are shown in Fig. 3. Each curve has a vertical asymptote defined by the flux linkage λ_m equal to $l_d i$, which implies that the center of the voltage ellipses falls exactly onto the current circle. The same value of λ_m individuates, for each ξ, the maxima of the curves in Fig. 2(a). Operation with λ_m lower than that of the asymptote is described by a circle diagram with the center of the ellipses inside the current circle, as in Fig. 1(a). An analysis of the position of the point P for different motor parameters, and the locus of the maximum torque-to-voltage ratio are presented in [14].

From Fig. 3 it can be observed that the maximum drive speed increases when the flux linkage decreases (with constant ξ) or when the saliency ratio decreases (with constant λ_m). In particular an SMD with an REL motor does not have a bounded speed, as discussed in [9] and [12]. Moreover one can realize that an infinite speed could be obtained also by an SPM motor, but this implies large motor inductances (that in general requires additional components external to the motor) and/or large current.

V. SMD FLUX-WEAKENING PERFORMANCE

With the purpose to derive an effective procedure for selecting the IPM motor parameters, this section investigates the performance of the class of IPM motor drives under operation in the flux-weakening region. All the drives have $t_b = 1, \omega_b = 1$ and $v = 1$, and thus they are characterized by a combination of parameters $l_d, l_q = \xi l_d, \lambda_m$, and by the current i as given in Fig. 2. On the basis of these motor parameters and current rating, and with the aid of the circle diagram of Fig. 1, the torque t_{fw}, at a prefixed flux-weakening speed ω_{fw}, is computed for each flux linkage λ_m and saliency ratio ξ. Since the analytical form of the torque is not available, because of the involved SMD equations (4)–(6), the results are shown graphically. For a practical use, some of them are reported in Fig. 4, where the achieved flux-weakening power $\omega_{fw} t_{fw}$ is reported as a function of λ_m and ξ, for different speed ω_{fw}. The performance of REL $(\lambda_m = 0)$ and SPM $(\xi = 1)$ motor drives will be further particularized in Section VI.

From Fig. 4 it can be noted that, for each saliency ratio ξ, a flux linkage λ_m exists, at which the flux-weakening power $\omega_{fw} t_{fw}$ is maximum. By comparing Fig. 4 and Fig. 2 one deduces that the flux-weakening maximum power is obtained with $\lambda_m = l_d i$, that is when the center of the voltage limit ellipses is exactly on the current limit circle. Moreover, the maximum value of the normalized power is approximately always the same, a little lower than $\sqrt{2}$ ($\sqrt{2}$ is the theoretical value with $\omega_{fw} = \infty$). Therefore, the corresponding maximum torque decreases when the speed ω_{fw} increases.

It can be noted also that, the flux-weakening power (and therefore torque) of an REL motor $(\lambda_m = 0)$ decreases for any given ξ, by increasing ω_{fw}. Similar behavior is exhibited by the flux linkage of a PM motor which assures the maximum flux-weakening power. In addition, by Fig. 4 and 2, it can be recognized that a wide flux-weakening speed range can also be obtained with low ξ, provided that high values of motor inductances or additional external phase inductances are accepted.

Eventually, by comparing the current values shown in Fig. 2 with the flux-weakening power shown in Fig. 4, one realizes that it is always preferable to design the synchronous motor with $\lambda_m > l_d i$; therefore, as far as the current is concerned, PM motors rather than REL motors should be preferred.

The design of the synchronous motor for flux-weakening applications can be described in the following steps. With the desired values of flux-weakening operating speed ω_{fw} and torque t_{fw}, suitable PM flux linkage λ_m and saliency ratio ξ are chosen, by using Fig. 4. The choice can be addressed by considering the preferences of the designer for the motor type and by practical considerations (see Appendix). Then, the corresponding l_d (and l_q) and drive current i can be determined by Fig. 2.

Some examples of SMD design are given in Table I for $t_{fw} = 0.2$ and $\omega_{fw} = 4, (\omega_{fw} t_{fw} = 0.8)$ and, of course, $t_b = 1, \omega_b = 1, v = 1$. The corresponding torque-speed and power-speed characteristics are shown in Fig. 5. The last column of the table specifies whether the center of the voltage limit ellipses is outside the current limit circle or not. The table

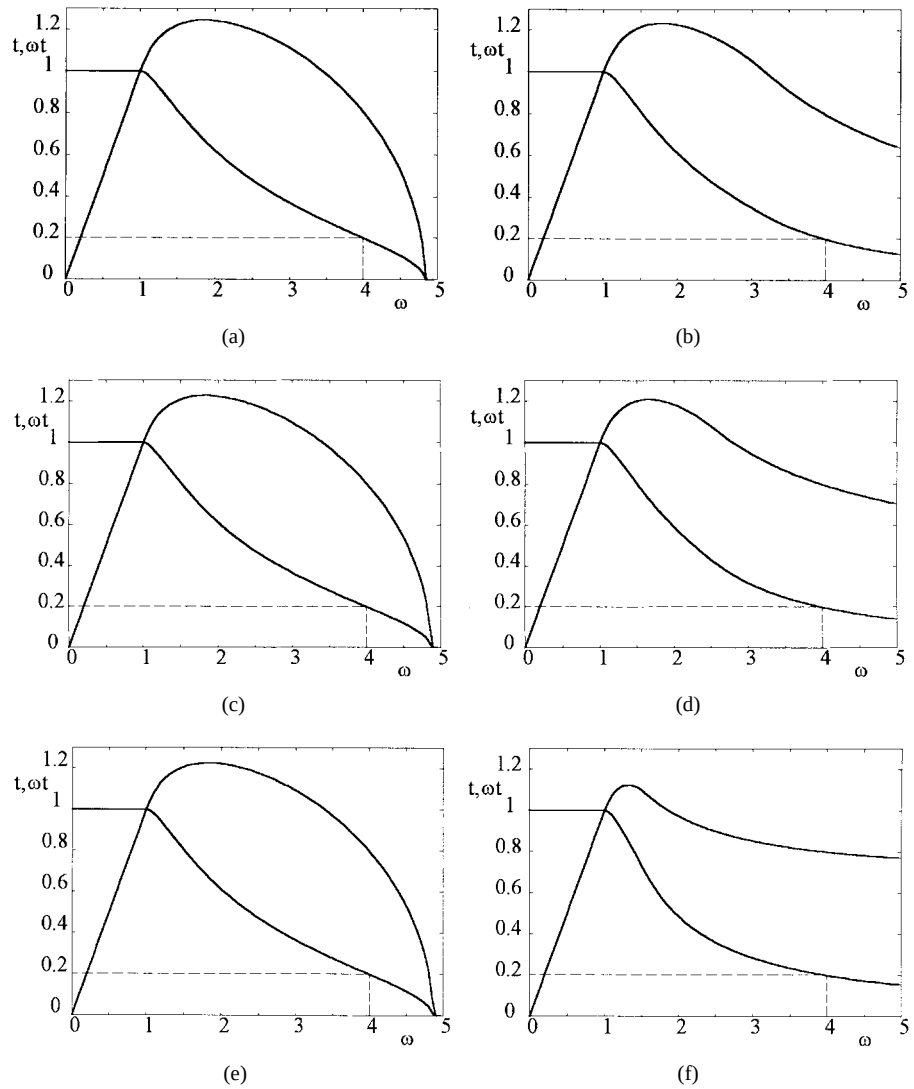

Fig. 5. Torque-speed and power-speed characteristics of the IPM motor drives of Table I.

suggests the following considerations.

- For PM motors, two different solutions are possible, with two different λ_m and same ξ (only the solution with higher λ_m is reported for the SPM motor).
- PM motors with higher λ_m have a lower rated current, approximately the same for all of them.
- PM motors have lower current than REL motors. By increasing ξ above the value of the table, REL motors exhibit higher t_{fw} and lower i, the latter remaining in any case higher than $\sqrt{2}$. However, REL motors with linear magnetic circuits are considered here. An improvement of the motor performance can be achieved taking advantage of iron saturation [16].
- The choice of $\lambda_m = l_d i$, which allows the highest flux-weakening power to be obtained, is not always the best one. In fact, if high torque t_{fw} is not required, the motor can be designed with a higher PM flux linkage λ_m, which permits the appreciable advantage of a lower rated drive current.
- Finally, one has to verify if the selected values of the d- and q-axis motor inductances are practicable or inductances external to the motor have to be connected. On the other hand, the flux linkage is in general easily obtained.

VI. Particular Cases

A. Synchronous Reluctance Motor

In an REL motor, the PM flux linkage is zero. Then, from (6), the maximum torque-to-current ratio angle is $\gamma_b = 45°$. By putting this angle in (4) and (5) together with $t_b = 1, v = 1$, and $\omega_b = 1$, the normalized values of the d-q axis inductances and drive current can be analytically carried out as functions of the saliency ratio ξ

$$l_d = \frac{\xi - 1}{\xi^2 + 1} \quad l_q = \frac{\xi^2 - \xi}{\xi^2 + 1} \quad i = \frac{\sqrt{2(\xi^2 + 1)}}{\xi - 1}. \tag{8}$$

The trends of l_d and i given in (8) are shown in Fig. 6. The figure points out that l_d has a maximum value at $\xi = 1 + \sqrt{2}$, as can be proved by the first of (8). This justifies the behavior of l_d in Fig. 2(a) for $\lambda_m = 0$. Moreover, the same Fig. 6 shows that the rated current i is always higher than $\sqrt{2}$.

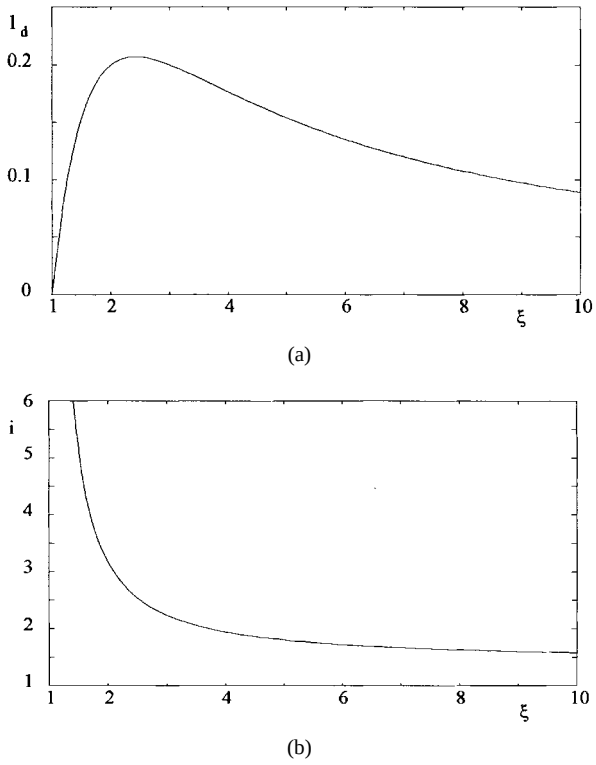

Fig. 6. d-axis inductance and rated current of an REL motor drive, as functions of ξ with the same base conditions of Fig. 2.

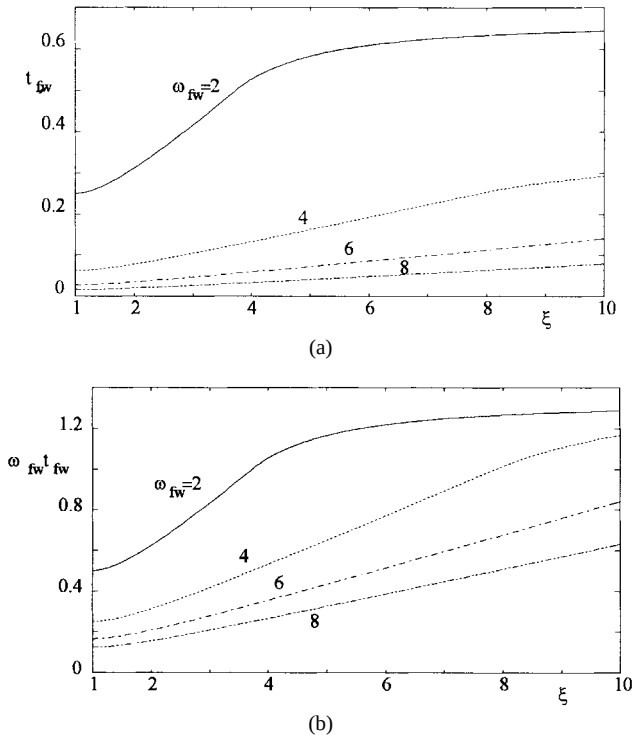

Fig. 7. Flux-weakening power and torque of the drive of Fig. 6, as functions of ξ and ω_{fw}.

With the same procedure used for deriving Fig. 4, the flux-weakening torque t_{fw} and power $\omega_{fw}t_{fw}$ with different values of ω_{fw} can be evaluated as functions of ξ. The results are reported in Fig. 7. From the figure, one observes that at any speed ω_{fw} the torque and power are always greater than zero. Moreover, it can be noted that both the maximum torque and power decrease with ω_{fw}, while in an IPM motor the maximum power can be kept constant, close to $\sqrt{2}$.

B. Superficial PM Motor

In an SPM motor, the d- and q-axis inductances assume identical values. Therefore the maximum torque-to-current ratio calls for an angle $\gamma_b = 0°$, that is, only q-axis current is supplied to the motor in the constant torque region. By fixing $t_b = 1$, $\omega_b = 1$, $v = 1$, and $\gamma_b = 0°$, the motor inductance and the drive current are obtained from (4) and (5) as functions of λ_m. They are

$$l_d = l_q = \lambda_m \sqrt{1 - \lambda_m^2} \qquad i = \frac{1}{\lambda_m}. \tag{9}$$

The inductances and current in (9) are reported in Fig. 8. With an SPM motor the maximum flux-weakening normalized speed $\omega_{\max}$ can be evaluated analytically in terms of the normalized flux linkage. Through (9) and (7) it results

$$\omega_{\max} = \frac{1}{\lambda_m - \sqrt{1 - \lambda_m^2}}. \tag{10}$$

From (10) one realizes that the speed is not limited if $\lambda_m \leq \sqrt{2}$, while if λ_m is higher than $\sqrt{2}$ the speed limit given by (10) applies.

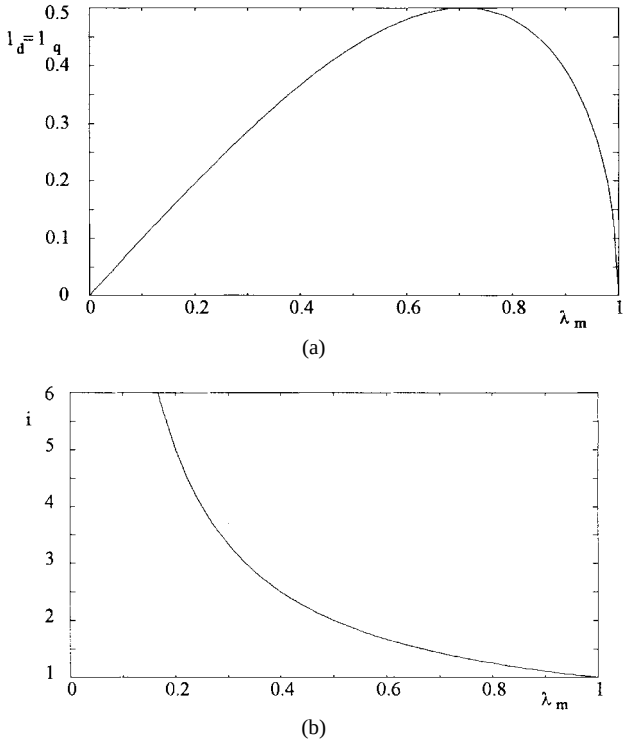

Fig. 8. Inductances and rated current of an SPM motor drive, as functions of λ_m with the same base conditions of Fig. 2.

Flux-weakening motor torque and power can be reported as functions of λ_m, for different values of ω_{fw}, as shown in Fig. 9. The figure points out that all the speeds ω_{fw} can be reached, even if high values of current or inductances may be required (see also Fig. 8) for the highest speed. Since high

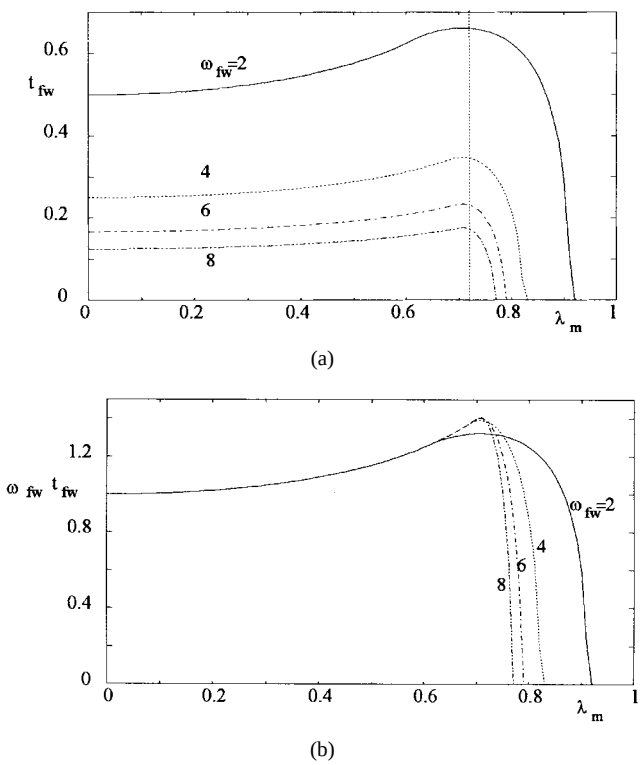

Fig. 9. Flux-weakening power and torque of the drive of Fig. 8, as functions of λ_m and ω_{fw}.

values of inductances are not earned by an SPM motor, a wide flux-weakening speed range calls for the use of external inductances. Moreover, it can be noted that the maximum power $\omega_{fw}t_{fw}$ does not decrease when w_{fw} increases (as it does in an REL motor). Its value is slightly lower than $\sqrt{2}$, while the maximum torque t_{fw} obviously decreases with speed.

VII. Conclusions

In this paper, the motor type and the related parameters as well as the inverter power rating of a synchronous motor drive (SMD) have been individuated, to meet a desired flux-weakening torque versus speed specification. At first, the normalized d-axis inductance l_d and rated current i are obtained, as functions of the normalized PM flux linkage λ_m and saliency ratio ξ, after the normalized base speed, rated torque, and voltage, have been fixed to unity. Then, by imposing the flux-weakening speed range and the torque limit at the highest flux-weakening speed, the appropriate combinations of λ_m and ξ are derived. The proposed method can be profitably used to design the most suitable SMD for given torque-speed performance, by an easy comparison of different solutions.

Appendix

The normalized quantities have been defined assuming as base torque T^*, speed Ω^*, and voltage V^*, the value they assume at the operating point B. Therefore $T^* = T_b, \Omega^* = \Omega_b, V^* = V$. As far as the motor parameters and current are concerned, their base values are fixed by considering an ideal REL motor having $L_d = 0, L_q = L^*$ and able to deliver the torque T^* with $I_d = I_q = I^*$. Then, the base current is given by $I^* = 2T^*\Omega^*/(3pV^*)$, while the base inductance is $L^* = 3pV^{*2}/(2\Omega^{*2}T^*)$. As a consequence base flux is $\Lambda_m^* = L^*I^* = V^*/\Omega^*$.

By applying the proposed normalization to the actual parameters of synchronous motors, their typical ranges result as follows.

An REL motor is characterized by its saliency ratio ξ, that strongly depends on the rotor structure. Generally, it ranges from 3 to 7 with the normalized l_q varying from 0.3 to 0.9 and i from about 3.2 to 1.7.

An SPM motor has a large and uniform equivalent airgap, since the PM relative permeability is near to unity. As a consequence the d- and q-axis inductances are equal and quite low. Typical normalized parameters of an SPM motor are $\lambda_m = 1 \div 0.95, l_d = l_q = 0.1 \div 0.3, i = 1 \div 1.1$

An IPM motor can present two different rotor configurations: with circumferentially magnetized PM and with radially magnetized PM. Their typical saliency ratios are $\xi = 1.5 \div 2.5$ and $\xi = 3 \div 6$, respectively. The flux linkage λ_m can be chosen from zero to one and consequently the inductances and current values vary from those of an REL motor to those of an SPM one.

References

[1] B. Sneyers, D. W. Novotny, and T. A. Lipo, "Field weakening in buried permanent magnet AC motor drives," *IEEE Trans. Ind. Applicat.*, vol. 21, pp. 398–407, Mar./Apr. 1985.
[2] T. M. Jahns, G. B. Kliman, and T. W. Neumann, "Interior permanent-magnet synchronous motors for adjustable-speed drives," *IEEE Trans. Ind. Applicat.*, vol. 22, pp. 738–747, July/Aug. 1986.
[3] T. M. Jahns, "Flux-weakening regime operation of an interior permanent-magnet synchronous motor drive," *IEEE Trans. Ind. Applicat.*, vol. 23, pp. 681–689, July/Aug. 1987.
[4] T. Sebastian and G. R. Slemon, "Operating limits of inverter-driven permanent magnet motor drives," *IEEE Trans. Ind. Applicat.*, vol. 23, pp. 327–333, Mar./Apr. 1987.
[5] R. F. Schiferl and T. A. Lipo, "Power capability of salient pole permanent magnet synchronous motors in variable speed drive applications," *IEEE Trans. Ind. Applicat.*, vol. 26, pp. 115–123, Jan./Feb. 1990.
[6] S. Morimoto, Y. Takeda, T. Hirasa, and K. Taniguchi, "Expansion of operating limits for permanent magnet motor by current vector control considering inverter capability," *IEEE Trans. Ind. Applicat.*, vol. 26, pp. 866–871, Sept./Oct. 1990.
[7] A. K. Adnanes, "Torque analysis of permanent magnet synchronous motors," in *Proc. Power Electron. Specialist Conf.*, 1991, pp. 695–701.
[8] A. K. Adnanes and T. M. Undeland, "Optimum torque performance in PMSM drives above rated speed," in *Ind. Applicat. Soc. Annu. Meet. Rec.*, 1991, pp. 169–175.
[9] R. E. Betz, "Control of Synchronous Reluctance machines," in *Ind. Applicat. Soc. Annu. Meet. Rec.*, 1991, pp. 456–462.
[10] R. E. Betz, M. Javanovic, R. Lagerquist, and T. J. E. Miller, "Aspects of the control of synchronous reluctance machines including saturation and iron losses," in *Ind. Applicat. Soc. Annu. Meet. Rec.*, 1992, pp. 456–463.
[11] B. J. Chalmers, "Influence of saturation in brushless permanent-magnet motor drives,"*Proc. Inst. Elec. Eng.*,vol. 139,pt. B,pp. 51–52,Jan. 1992.
[12] W. L. Soong and T. J. E. Miller, "Theoretical limitations to the field-weakening performance of the five classes of brushless synchronous AC motor drive," in *Proc. Elec. Machines and Drives Conf.*, Oxford, U.K., 1993, pp. 127–132.
[13] ——, "Practical field-weakening performance of the five classes of brushless synchronous AC motor drive," in *Proc. European Power Electron. Conf.*, Brighton, U.K., 1993, pp. 303–310.
[14] N. Bianchi and S. Bolognani, "Design considerations about synchronous motor drives for flux weakening applications," in *Proc. Symp. Elec. Drives Design Applicat.*, Lausanne, Switzerland, 1994, pp. 185–190.
[15] ——, "Design procedure of a synchronous motor for flux-weakening operation," in *Proc. Symp. Elec. Drives Design Applicat.*, Nancy, France, 1996, pp. 235–240.
[16] ——, "Synchronous reluctance motor drives: Overload and flux-weakening performance taking into account iron saturation," in *Int. Conf. Elec. Machines*, Vigo, Spain, 1996, pp. 360–365.

Nicola Bianchi was born in Verona, Italy, on January 18, 1967. He received the laurea degree in electrical engineering from the University of Padova, Italy, in 1991, with a thesis rewarded by AEI (Italian Electrotechnics and Electronics Association). After that, he joined the Electric Drives Laboratory at the Department of Electrical Engineering of the University of Padova, as a Ph.D. student. He received the Ph.D. degree in electrical engineering in 1995. Currently, he is a Post-Doctorate Student at the same laboratory.

He is involved in the design of ac permanent magnet, reluctance, and induction motors with particular interest in drive applications.

Silverio Bolognani is a native of Trento Province, Italy. He received the laurea degree in electrical engineering from the University of Padova, Italy, in 1976.

He joined the Department of Electrical Engineering at the same university, where he was involved in the analysis and design of thyristor converters and synchronous motor drives. After that, he started the Electrical Drives Laboratory and he carried out research on brushless and induction motor drives. He is presently an Associate Professor of electrical drives and he is engaged in research on advanced control techniques for motor drives and motion control and on design of ac electrical motors for variable-speed applications. He is author of more than 80 papers on electrical machines and drives.